HHS Public Access

Author manuscript

*J Pharm Pharmacol*. Author manuscript; available in PMC 2018 December 20.

Published in final edited form as:

*J Pharm Pharmacol*. 2016 September ; 68(9): 1203–1213. doi:10.1111/jphp.12592.

# Chlorogenic acid inhibits cholestatic liver injury induced by α-naphthylisothiocyanate: involvement of STAT3 and NFκB signalling regulation

**Zhen Tan**[a], **Min Luo**[b], **Julin Yang**[c], **Yuqing Cheng**[a], **Jing Huang**[b], **Caide Lu**[b], **Danjun Song**[b], **Meiling Ye**[a], **Manyun Dai**[b], **Frank J. Gonzalez**[d], **Aiming Liu**[b], and **Bin Guo**[a]

[a]Key Laboratory of Phytochemical R&D of Hunan Province, Hunan Normal University, Changsha,

[b]Medical School of Ningbo University,

[c]Ningbo College of Health Sciences, Ningbo, China

[d]Laboratory of Metabolism, National Cancer Institute, NIH, Bethesda, MD, USA

## Abstract

**Objectives—**Chlorogenic acid (CGA) is one of the most widely consumed polyphenols in diets and is recognized to be a natural hepatoprotective agent. Here, we evaluated the protective effect and the potential mechanism of CGA against α-naphthylisothiocyanate (ANIT)-induced cholestasis and liver injury.

**Methods—**Twenty-five male 129/Sv mice were administered with CGA, and ANIT challenge was performed at 75 mg/kg on the 4th day. Blood was collected and subjected to biochemical analysis; the liver tissues were examined using histopathological analysis and signalling pathways.

**Key findings—**Chlorogenic acid almost totally attenuated the ANIT-induced liver damage and cholestasis, compared with the ANIT group. Dose of 50 mg/kg of CGA significantly prevented ANIT-induced changes in serum levels of alanine aminotransferase, alkaline phosphatases, total bile acid, direct bilirubin, indirect bilirubin (5.3-, 6.3-, 18.8-, 158-, 41.4-fold, $P<0.001$) and aspartate aminotransferase (4.6-fold, $P<0.01$). Expressions of the altered bile acid metabolism and transport-related genes were normalized by cotreatment with CGA. The expressions of interleukin 6, tumour necrosis factor-α and suppressor of cytokine signalling 3 were found to be significantly decreased (1.2-fold, ns; 11.0-fold, $P<0.01$; 4.4-fold, $P<0.05$) in the CGA/ANIT group. Western blot revealed that CGA inhibited the activation and expression of signal transducer and activator of transcription 3 and NFκB.

**Conclusions—**These data suggest that CGA inhibits both ANIT-induced intrahepatic cholestasis and the liver injury. This protective effect involves downregulation of STAT3 and NFκB signalling.

**Correspondence** Aiming Liu, Medical School of Ningbo, University, Ningbo 315211, China. liuaiming@nbu.edu.cn and Bin Guo, Hunan Normal University, Changsha 410081, China. binguo@hunnu.edu.cn.

Declarations

Conflict of interest

The authors declared that they have no conflicts of interest to disclose

**Keywords**

chlorogenic acid; cholestasis; NFκB; STAT3; α-naphthylisothiocyanate

## Introduction

Cholestasis is a condition defined as a defective bile acid flow from the liver to the duodenum, due to the obstruction of bile ducts, impaired bile formation or secretion induced by drugs, infections, metabolic or genetic disorders.[1] On a mechanistic basis, cholestasis is generally classified into extra- and intrahepatic forms.[2] On a clinical basis, cholestasis is characterized by an elevation in the level of serum alkaline phosphatase (ALP) and total bile acid (TBA), which often precede the development of jaundice and parenchyma injury in the liver. Owing to nutritional problems and liver injury caused by the accumulation of toxic compounds,[2] cholestasis is an important manifestation of inherited and acquired liver diseases.[3,4] However,many liver diseases due to cholestasis have not been curedand still lack an effective pharmacotherapy [5,6] and cholestasis progresses towards hepatic fibrosis, cirrhosis and liver failure without proper treatment.[7,8]

Cholestasis induced by α-naphthylisothiocyanate (ANIT) is the most used experimental model. In this model, cholangiolitic hepatitis was characterized by intrahepatic cholestasis, biliary epithelial cell necrosis, bile duct obstruction and then hepatocellular injury.[9–11] These characteristics mimic the drug-induced cholestasis and hepatic injury in humans. Therefore, treatment with ANIT is used as a typical protocol to prepare intrahepatic cholestasis model, which was used in this study.

At present, traditional phytotherapy and plant-derived natural medicine are quite popular for treating liver diseases. Lonicera japonica Thunb (Caprifoliaceae family), known as Jinyinhua (in Chinese), is widely consumed as healthy tea beverage and used in traditional Chinese medicine (TCM) to treat various diseases including hepatitis, arthritis, allergy and infection. [12–16] Of particular interest is the *L. japonica*-containing TCM formula: Yin-zhi-huang (YZH) is a classical polyherbal prescription dated from the traditional Chinese prescription ‘Yin-chen-hao-tang’,[17,18] which has been widely used in East Asian countries for more than a thousand years to treat jaundice and chronic liver diseases.[19,20] Extensive studies on the phytochemical ingredients from coffee and *L. japonica* demonstrated that chlorogenic acid (CGA) is supposed to be the primary active component (indicator compound) contributing to the health benefits.[13,14,19]

Chlorogenic acid (5’-caffeoylquinic acid, Figure 1) is one of the most dietary polyphenols found in fruits, vegetables and plant-derived traditional medicines.[20,21] It was reported that the antioxidant activity of CGA may reduce the risk of some chronic diseases.[19,22,23] Some studies have shown that CGA is the anti-inflammatory compound in CGA-containing natural products.[10,21] Importantly, CGA has been reported to be biologically active to protect against experimental liver injuries.[24–26] A recent study of CGA reported its protective effect against liver injury caused by bile duct ligation, involving transcriptional regulation of collagen and growth factor expression.[27] However, no effect of CGA action on bile acid

metabolism and cholestatic inflammation was found in previously reported intrahepatic cholestasis models.

Lately, several bioactive compounds from medical herbs are reported to exhibit a remarkable chemopreventive activity against drug-induced cholestasis, liver injury, hepatotoxicity and digestive disorders via regulating inflammatory signalling pathways.[28–31] For example, emodin from *Rheum officinale* is used to treat digestive disorders, shows a hepatoprotective effect and prevents cholestatic hepatitis *via* anti-inflammatory process.[28] Resveratrol, a dietary polyphenol present in peanuts, grapes and red wine, exerts a hepatoprotective effect against paracetamol-induced liver injury by regulating SIRT-p53 signalling pathways.[30] Some of the protective effects involve NFκB or STAT3 signalling pathways that are critically important in cell survival and apoptosis. Isoquercitrin protected against paracetamol-induced liver injury; the anti-inflammatory activity of isoquercitrin occurs through the blockade of NFκB and MAPK signalling pathways.[32] Plumbagin ameliorates $CCl_4$-induced hepatic fibrosis in rats through the down-regulation of EGFR and STAT3 in the liver.[33] Saikosaponin D, one of the major bioactive components of the Chinese herb *Bupleurum falcatum*, was found to protect mice from paracetamol-induced hepatotoxicity by inhibiting NFκB and STAT3 signalling pathways.[29] However, involvement of NFκB and STAT3 in protection against cholestasis by CGA has not ever been reported.

This work aimed to evaluate the protective effects of CGA against intrahepatic cholestasis and hepatotoxicity induced by ANIT in mice. The underlying mechanism involving repressing NFκB activation and inhibiting STAT3 signalling was also investigated, in combination with a systematic assessment of CGA exposure, biochemical and histopathological changes, expressions of inflammatory cytokines.

## Materials and Methods

### Chemicals and reagents

Chlorogenic acid (98%, Figure 1a) was obtained from the National Institute for the Control of Pharmaceutical and Biological Products (Beijing, China). α-Naphthyl isothiocyanate (ANIT, 95%) was purchased from Sigma Aldrich (Louis, MO, USA). Trizol was provided by Invitrogen (Carlsbad, CA, USA). Alkaline phosphatase (ALP), alanine aminotransferase (ALT), aspartate aminotransferase (AST), total bile acid (TBA), direct bilirubin (DBIL) and indirect bilirubin (IBIL) assay kits were from Yonghe Sunshine Technology (Changsha, China). Antibodies against NFκB subunit p65 and active form p-p65, total STAT3 (t-STAT3) and phospho-STAT3 (p-STAT3) were purchased from Cell Signaling (Danvers, MA, USA). Antibody against GAPDH was purchased from Abcam (Cambridge, MA, USA). Ultrapure water was freshly prepared using a Milli-Q50 SP Reagent Water System (Bedford, MA, USA). All the other chemicals were of the highest grade from commercial sources.

### Animal and treatment

Twenty-five male 129/Sv mice (5 weeks old, 20 ±5 g) were provided by the Experimental Animal Center, Ningbo University, and housed in plastic cages under controlled humidity (average 55%) and temperature (average 25 °C). The mice were exposed to a 12-h light/dark

cycle with free access to purified water and a standard diet. Animal handling and experimental procedures were approved by the Ethics Committee of Medical School of Ningbo University and were conducted in accordance with the Guide for the Care and Use of Laboratory Animals.

Twenty mice were divided into four groups ($n$ = 5): control, CGA, ANIT and CGA/ANIT. CGA and ANIT were dissolved in corn oil. The mice in the CGA and CGA/ANIT groups were gavaged with CGA 50 mg/kg once daily for 5 days. On the 4th day, the ANIT and CGA/ANIT groups were orally administered ANIT 75 mg/kg.[34] The vehicle/ control group was fed vehicle only. Two days after the ANIT challenge, the mice were weighed and killed by taking off the neck to death after blood collection. The serum samples were centrifuged at 3000 rpm for 10 min, and the supernatants were collected. Liver tissues were harvested and weighed to calculate liver/body weight ratio. A section of freshly isolated liver tissues was excised and immediately fixed in 10% neutral buffered formalin after a brief wash with phosphate-buffered saline. The remaining liver tissues were flash-frozen in liquid nitrogen and then stored at 80 °C until analysis.

## Serum chlorogenic acid exposure measurement

To measure the systemic serum concentration of CGA, the rest five mice were intragastrically treated with single dose of 50 mg/kg b.w. CGA once; 0.5, 1, 2, 5, 24, 48 and 72 h after dosing, the blood was collected from the tail vein. A volume of 50 μl serum was isolated by centrifuging the blood at 3000 rpm for 10 min, and 100 μl acetonitrile was added. The mixture was vortexed for 30 s and centrifuged at 15 000 g for 20 min. An aliquot of 10 μl supernatant was injected to a Shimadzu high-performance liquid chromatography (HPLC) system (Kyoto, Japan) coupled with an API-4000 triple quadrupole mass spectrometer (Toronto, Canada). The ion transition of m/z 353.2→191.4 was detected in multiple reaction monitoring mode with negative electrospray ionization (ESI). A calibration curve with correlation coefficient ($r^2$) above 0.99 was constructed for quantification.

## Biochemical assay

The serum samples were haemolysis-free and stored at 20 °C before determining the biochemical parameters. The alanine aminotransferase (ALT), aspartate aminotransferase (AST), alkaline phosphatase (ALP), total bile acid (TBA), direct bilirubin (DBIL) and indirect bilirubin (IBIL) in the serum samples were assayed by Spectra Max M5 (Sunnyvale, CA, USA).

## Histopathological and apoptosis assessments

Fixed liver tissues were dehydrated in a serial concentration of alcohol and xylene, embedded in paraffin and cut into four-micrometre serial sections. The sections were stained with haematoxylin and eosin for histopathological examination and examined using Olympus BX41 light microscope. For apoptotic analysis, the sections were stained with 4’,6-diamidino-2-phenylindole (DAPI) and examined under fluorescence microscope. The positive rate of four groups was calculated and compared.

### Quantitative-PCR analysis

Total RNA from mice hepatic tissues homogenized in Trizol reagent was determined by Nano Drop 2000 (Thermo Fisher, Waltham, MA, USA). Reverse transcription was performed with M-MLV Reverse Transcriptase. Reaction volume (20 μl) included 59 reaction buffer, 10 mM dNTPs, 1 μg oligo dT18, 1 μg random primer, 1 μg total RNA, 200 U M-MLV and 20 U RNasin. The procedure was conducted according to the manufacturer's protocol. The synthesized cDNA was stored at −20 °C until analysis.

The primer sequences listed in Table 1 were extracted from the public database (http://mouseprimerdepot.nci.nih.gov/). Each 10 μl PCR reaction mixture contained 1 μl total cDNA, 5 μl LightCycle 480 SYBR Green I Master Mix (FastStart Taq DNA Polymerase, reaction buffer, dNTPmix, SYBR Green I dye and $MgCl_2$), 0.2 μl forward primer, 0.2 μl reverse primer and 3.6 μl nuclease-free water. Amplification with 35–40 cycles was performed: reaction cycle consisting of denaturation at 95 °C for 10 s, renaturation at 55 °C for 10 s and then elongation at 72 °C for 15 s. The fluorescence signal was detected at the end of each cycle, and 18S rRNA was used as an internal control. Melting curve analysis was used to confirm the specificity of the primers.

### Western blot analysis

Liver tissues were homogenized by MagNA Lyser (Roche) using RIPA buffer (1 : 10, g/v) containing 1% PMSF (Shanghai, China). Tissue debris was removed by centrifugation at 10 000 g and 4 °C for 5 min. The total protein was quantified using a BCA protein assay kit from Beyotime Biotech Co. Ltd (Nantong, China). To each tube, an equivalent volume of 5× SDS-PAGE sample loading buffer (Shanghai, China) and the proteins were boiled for 5 min. The samples were loaded and separated on 10% SDS–poly-acrylamide electrophoresis gels.

The proteins were transblotted onto PVDF membranes that were blocked with 5% fat-free milk at 37 °C for at least 2 h. The membranes were incubated overnight with primary antibodies against p65, p-p65, p-STAT3, t-STAT3 and GAPDH. After secondary antibody incubation for 2 h, the blotted membranes were exposed to ECL substrates Advansta (Menlo Park, CA, USA), and the signals were detected by Kodak X-ray films (Rochester, NY, USA). Densitometry analysis was performed, and the result was expressed as the relative intensity of p-STAT3, t-STAT3, p-p65 and p65 vs GAPDH, respectively.

### Statistical analysis

All data were averaged from five independent experiments ($n = 5$) and were expressed as mean ± SD. Nonparametric Kruskal–Wallis test was performed where the difference between the four groups in all the biomarkers was determined significant ($P < 0.05$) and post hoc test between treatments was performed. Then, comparison of CGA and ANIT groups with the control indicated the toxic potential of CGA and success of positive model. Comparison between ANIT and CGA/ANIT groups was made to check the protective effect by CGA where $P < 0.05$ was considered significant.

## Results

### Serum chlorogenic acid exposure

The MRM transition of CGA was determined as 353.2→ 191.4 in ESI¯mode with the fragmentation pattern shown in Figure 1a. The HPLC-MRM data demonstrated a linear relationship with $r^2 > 0.99$. In the single-dose group, after the administration of 50 mg/kg of CGA, the serum concentration of CGA was determined to be above 5 ng/ml for 5 h and disappeared after 24 h (Figure 1b). The serum concentration of CGA in the consecutive dose group was around 1.5 ng/ml.

### Hepatic biochemistry

Serum ALT and AST are reliable indicators of acute hepatic injury. As shown in Figure 2a and 2b, both serum ALT and AST levels were found to be significantly increased (5.3fold, $P < 0.001$; 4.6-fold, $P < 0.01$) in the ANIT-treated group, in comparison with the control group. The increase in ALT and AST was attenuated by pretreatment with CGA at 50 mg/kg ($P < 0.01$), suggesting an evident protection effect of CGA.

Alkaline phosphatase and TBA are typical indicators of intrahepatic cholestasis. Similar to the ALT and AST analyses, ALP and TBA levels were found to be significantly increased (6.3- and 18.8-fold, $P < 0.001$) in the ANIT group. In the CGA/ANIT group, they were found to be significantly decreased ($P < 0.01$, $P < 0.001$). A notable protective effect was produced by pretreatment with CGA (Figure 2c and 2d).

Direct bilirubin and IBIL are two toxic indicators closely associated with cholestasis. In this study, serum DBIL and IBIL levels were found to be elevated (158- and 41.5-fold, $P < 0.001$) in the ANIT group. Administration of CGA totally attenuated ($P < 0.01$) the ANIT-induced increase in DBIL and IBIL activity (Figure 2e and 2f).

### Histopathological and apoptosis analyses

Pathological analysis revealed that 75 mg/kg ANIT resulted in necrosis and infiltration of neutrophils and monocytes in the ANIT group (Figure 3e and 3f). In contrast, only small lesions were observed sporadically under the low-power microscope, indicating that liver damage was attenuated in the CGA/ANIT group (Figure 3g). In the control and CGA groups, the liver tissues were histologically normal (Figure 3a and 3c), revealing no hepatotoxicity by treatment with CGA alone. Thus, pretreatment with 50 mg/kg CGA protected mice against ANIT-induced liver injury. By DAPI staining of the nuclei to check the involvement of apoptosis, no significant increase in positive staining was observed between the treatments specified (data not shown).

### Influence of chlorogenic acid on bile acid metabolism and transportation

The rate-limiting enzymes CYP7A1, CYP8B1 and CYP27A1 play a key role in bile acid homeostasis. *Cyp7a1*, *Cyp8b1* and *Cyp27a1* mRNAs were found to be increased (4.9-, 4.8- and 1.4-fold, $P < 0.05$, Figure 4a) in the ANIT group, while in the CGA/ANIT group, their expression was found to be reversely regulated and almost normalized by pretreatment with CGA.

Basolateral efflux transporters MRP3 and MRP4 are involved in the export of bile acids to the blood. Multidrug resistance-related protein 2 (MRP2), bile salt export pump (BSEP) and organic solute transporter-β (OSTB) export bile acids into canaliculi. *Ostb*, *Mrp2* and *Mrp3* mRNAs increased (12.3-, 3.2- and 3.7-fold, $P < 0.05$) in the ANIT-treated group; similar changes were observed for *Bsep* and *Mrp4* mRNAs. These data were in accordance with a previous report.[35] In this study, the expression of these mRNAs was normalized by treatment with CGA (Figure 4b).

The basolateral transporters such as organic anion-transporting polypeptide 1 (OATP1), organic anion-transporting polypeptide 2 (OATP2) and sodium/taurocholate-cotransporting polypeptide (NTCP) are involved in the bile acid uptake. *Oatp2* and *Ntcp* mRNA expression decreased (1.1fold, ns; 1.2-fold, $P < 0.05$) after ANIT (75 mg/kg) challenge, while the expression of *Oatp1* mRNA was found to be increased in the vehicle/ANIT group (Figure 4c). In the CGA/ANIT group, all mRNAs returned to the baseline levels.

## Effects of chlorogenic acid on inflammation, necrosis and apoptosis

Because inflammation often occurs when the liver is injured by toxins, mRNAs of typical genes involved in inflammation, such as *Il-6* and Tnf-α, were analysed. Compared with the control group, expressions of *Il-6* and Tn*f*-α mRNAs were found to be significantly increased (39-fold, $P < 0.05$; 11-fold, $P < 0.01$) in the ANIT group. However, transcription factors *c-Fos* and *c-Jun* mRNAs were found to be not changed between those groups. These data indicate that the proinflammatory *Il*-6 and TNF-α have an important role in intrahepatic cholestasis (Figure 5a).

Target genes of STAT3, including *Fga*, *Fgb*, *Fgg* and *Socs3*, are often involved in toxicity.[29] In this study, *Fga*, *Fgb*, *Fgg* and *Socs3* mRNAs were found to be significantly increased 3.1-, 2.0-, 9.5- and 16.1-fold in the ANIT group compared with vehicle alone. In contrast, these mRNAs were lower in the CGA/ANIT group except for *Fgb*, indicating the potential role for STAT3 in ANIT-induced cholestasis (Figure 5b).

*Fas*, *ICE* and *Bcl*-2 mRNAs encoding proteins involved in apoptosis were also measured in this study. *Fas* and *ICE* mRNAs were found to be increased after the administration of ANIT, but their levels were not decreased by pretreatment with CGA. Moreover, expression of *Bcl-2* mRNA was not different between these groups, suggesting that apoptosis is not involved in ANIT-induced liver injury (Figure 5c).

LXR and FXR are reported to regulate the expression of bile acid synthesis enzyme CYP7A1.[36,37] Considering the regulation of *Cyp7a1* in CGA group, the involvement of LXR and FXR in the protection was checked by examining their target genes. No significant change in the LXR target genes *Abca1*, *Srebp* and *Lxr* was observed between these groups (Figure 5d). The expression of *Shp* mRNA increased after treatment with ANIT and was suppressed by CGA, which was in accordance with the previous report.

## Activation and expression of STAT3 and NFκB

STAT3 is a master regulator of genes involved in inflammation. The active form p-STAT3 increased (5.0-fold, Figure 6b) in the ANIT group and was attenuated by coadministration of

CGA 50 mg/kg. Similarly, the total STAT3 increased moderately (1.5-fold, Figure 6b) in the ANIT group and decreased in the CGA/ANIT group (Figure 6). Thus, the protective effect of CGA against ANIT toxicity was associated with the inhibition of both activation and expression of STAT3.

Compared with the ANIT group, the protein level of p-p65 and p65 showed a moderate decrease in CGA/ANIT group. In the CGA group, the total NFκB was not significantly affected, but a sharp decrease in p-p65 was observed (Figure 6a and 6c). These data indicated that the inhibition on NFκB activation was involved in the protection of CGA against ANIT toxicity.

## Discussion

Chlorogenic acid, an abundant component of *Yin-zhihuang*, was considered the major component in Jinyinhua (*Lonicerae Japonicae Flos*).[38] In the C57BL/6J mouse, CGA exhibited a significant protective effect against LPS-induced liver toxicity when the mice were administered with 50 mg/ kg of CGA once daily for 5 days.[39] CGA efficiently inhibited $CCl_4$-induced liver fibrosis in rats when 60 mg/kg of CGA was intraperitoneally injected.[40] In a previous report, when Sprague-Dawley rats were intravenously administered YZH injection (1 ml/kg, equivalent to CGA 54 mg/kg), the plasma concentration of CGA was determined as 20 ng/ml 3 h after injection. In this study, the mice were treated with 50 mg/kg CGA and the steady-state serum concentration of CGA was determined to be above 5 ng/ml for at least 5 h. Clinically, YZH injection (10–20 ml) is administered once daily for neonatal jaundice or cholestasis, and the dose is equivalent to CGA 54–108 mg/kg in mouse. Thus, the dose of CGA and its protective effect in this study were of relevance to medical application.

α-naphthylisothiocyanate causes cholestasis by injuring the bile duct epithelial cells, and the rodents treated with ANIT are commonly used as animal models to emulate human intrahepatic cholestasis for elucidating the mechanism of this drug-induced cholestatic liver injury.[6,41] In this study, bile acid synthesis genes *Cyp7a1*, *Cyp8b1*, *Cyp27b1* decreased after gavaged with ANIT for 48 h. Hepatic basolateral and canalicular transporters were found to be increased in the ANIT group. Transporters involved in bile acid uptake decreased after the administration of ANIT. In contrast, expressions of the bile acid metabolism and transport-related genes altered by ANIT were normalized by cotreatment with CGA. These modifications could not explain the increased TBA by ANIT treatment. Based on the analysis of the FXR target SHP whose suppressive role is associated with FXR signalling,[42–44] the alteration in bile acid metabolism seemed secondary to the attenuated toxicity.

In the progression of xenobiotic-induced hepatotoxicity and liver disease, it is generally accepted that inflammation plays a critical role.[29,36–38] In LPS-induced liver injury mouse model, the hepatic expressions of toll-like receptor 4 (*Tlr4*), *Tnf-α* and *NFκB p65* subunit mRNAs were found to be increased after the LPS challenge.[39] TNF-α is the key pro-inflammatory cytokine that initiates the inflammatory response and induces massive apoptosis of hepatocytes.[45] In the present study, after the administration of 75 mg/kg

ANIT, the inflammatory factors IL-6 and TNF-α mRNAs were found to be significantly increased and attenuated by pretreatment with CGA. Thus, the anti-inflammatory activity of CGA may play a key role in the protection against the liver injury induced by ANIT.

Recent studies revealed that a prophylactic injection of IL-22, a STAT3-activating cytokine, significantly reduced serum ALT levels and histopathological damage in the APAP-induced liver injury, suggesting a protective role of STAT3.[46] Alisol B 23-acetate produced a protective effect against $CCl_4$-induced hepatotoxicity, while alisol B 23-acetate induced the expression of STAT3 phosphorylation and STAT3 target genes *Bcl-xl* and *Socs3*, resulting in decreased hepatocyte apoptosis.[7] In this study, transcription of apoptotic and anti-apoptotic genes was not modified (Figure 5), which correlated with the DAPI staining result (data not shown). So apoptosis pathway was not involved in the toxicity or the protection process. However, STAT3 target genes *Socs3*, *Fga*, *Fgb* and *Fgg* mRNAs were found to be increased in the ANIT group and normalized in CGA/ANIT group. Considering the modified activation and expression of STAT3 by CGA treatment, STAT3 was supposed to play a key role in intrahepatic cholestasis induced by ANIT.

The typical inflammatory factors TNF-α and IL-6 are mostly related to the activation of the NFκB pathway. In this study, they were found to be up-regulated in ANIT group and decreased by the treatment of CGA. In addition to the decrease in p-p65 and p65 in CGA/ANIT group, CGA treatment caused a sharp decrease in p-p65 CGA group, which was unlike that of STAT3. Thus, the NFκB pathway was likely involved in the protection against intrahepatic cholestasis by CGA.

## Conclusion

In conclusion, CGA, a major active component of functional foods and herbal medicines, was found to protect against ANIT-induced hepatotoxicity involving the inhibition of STAT3 and NFκB signalling. The data provided new insights into the chemopreventive effects of CGA-containing herbal formula, such as the traditional Chinese medicine YZH, against cholestasis in East Asian countries. CGA, as an active chemical entity from traditional medicines, demonstrated the promising characteristics of a potential candidate to be developed.

## Acknowledgements

This work was financially supported by the National Natural Science Foundation of China (Grant No. 81274178, 81273582 and 81302848), Zhejiang Provincial Education Department (No. Y201329949), Foundation for University Young Key Teacher by the Education Department of Hunan Province and the Construct Program of the Key Discipline in Hunan Province. We greatly thank the technical support by Key Laboratory of Phytochemical R&D of Hunan Province and Key Laboratory of Chemical Biology and Traditional Chinese Medicine Research (Ministry of Education of China).

## References

1. Trauner M et al. Molecular pathogenesis of cholestasis. N Engl J Med 1998; 17: 1217–1227.
2. Koopen NR et al. Molecular mechanisms of cholestasis: causes and consequences of impaired bile formation. Biochim Biophys Acta 1998; 1: 1–17.

3. Watanabe N et al. Clinical and pathological features of a prolonged type of acute intrahepatic cholestasis. Hepatol Res 2007; 8: 598–607.
4. Padda MS et al. Drug-induced cholestasis. Hepatology 2011; 4: 1377–1387.
5. Carey EJ, Lindor KD. Current pharmacotherapy for cholestatic liver disease. Expert Opin Pharmacother 2012; 17: 2473–2484.
6. Yang F et al. Evaluation of the protective effect of Rhei Radix et Rhizoma against alpha-naphthylisothiocyanate induced liver injury based on metabolic profile of bile acids. J Ethnopharmacol 2012; 3: 599–604.
7. Meng Q et al. Protective effects of alisol B 23-acetate from edible botanical Rhizoma alismatis against carbon tetrachloride-induced hepatotoxicity in mice. Food Funct 2015; 4: 1241–1250.
8. Boyer JL. New perspectives for the treatment of cholestasis: lessons from basic science applied clinically. J Hepatol 2007; 3: 365–371.
9. Zimmerman HJ. Drug-induced liver disease. Drugs 1978; 1: 25–45.
10. Kossor D et al. Temporal relationship of changes in hepatobiliary function and morphology in rats following α-naphthylisothiocyanate (ANIT) administration. Toxicol Appl Pharmacol 1993; 1: 108–114.
11. Roth RA, Dahm LJ. Neutrophil-and glutathione-mediated hepatotoxicity of a-naphthylisothiocyanate. Drug Metab Rev 1997; 1–2: 153–165.
12. Shang X et al. Lonicera japonica Thunb.: ethnopharmacology, phytochemistry and pharmacology of an important traditional Chinese medicine. J Ethnopharmacol 2011; 1: 1–21.
13. Xiao ZP et al. Molecular docking, kinetics study, and structure-activity relationship analysis of quercetin and its analogous as Helicobacter pylori urease inhibitors. J Agric Food Chem 2012; 42: 10572–10577.
14. He L et al. Transcriptome analysis of buds and leaves using 454 pyrosequencing to discover genes associated with the biosynthesis of active ingredients in *Lonicera japonica Thunb*. PLoS ONE 2013; 4: e62922.
15. Xiong J et al. Screening and identification of the antibacterial bioactive compounds from *Lonicera japonica* Thunb. leaves. Food Chem 2013; 1: 327–333.
16. Li J et al. Rapid preparative extraction and determination of major organic acids in honeysuckle (*Lonicera japon-ica* Thunb.) tea. J Food Compos Anal 2014; 2: 139–145.
17. Zhang A et al. An in vivo analysis of the therapeutic and synergistic properties of Chinese medicinal formula Yin-Chen-Hao-Tang based on its active constituents. Fitoterapia 2011; 8: 1160–1168.
18. Wang X et al. Pharmacokinetics screening for multi-components absorbed in the rat plasma after oral administration traditional Chinese medicine formula Yin-Chen-Hao- Tang by ultra performance liquid chromatography-electrospray ionization/ quadrupole-time-of-flight mass spectrometry combined with pattern recognition methods. Analyst 2011; 23: 5068–5076.
19. Tverdal A, Skurtveit S. Coffee intake and mortality from liver cirrhosis. Ann Epidemiol 2003; 6: 419–423.
20. Higdon JV, Frei B. Coffee and health: a review of recent human research. Crit Rev Food Sci Nutr 2006; 2: 101–123.
21. Burgos-Moron E et al. The coffee constituent chlorogenic acid induces cellular DNA damage and formation of topoisomerase I- and II-DNA complexes in cells. J Agric Food Chem 2012; 30: 7384–7391.
22. Ruhl CE, Everhart JE. Coffee and tea consumption are associated with a lower incidence of chronic liver disease in the United States. Gastroenterology 2005; 6: 1928–1936.
23. Shi H et al. Chlorogenic acid protects against liver fibrosis in vivo and in vitro through inhibition of oxidative stress Clin Nutr 2016; doi: 10.1016/j.clnu.2016.03.002.
24. Zhou Y et al. Chlorogenic acid from honeysuckle improves hepatic lipid dysregulation and modulates hepatic fatty acid composition in rats with chronic endotoxin infusion. J Clin Biochem Nutr 2016; 2: 146–155.
25. Feng Y et al. Chlorogenic acid protects d-galactose-induced liver and kidney injury via antioxidation and anti-inflammation effects in mice. Pharm Biol 2016; 6: 1027–1034.

26. Zhou Y et al. Chlorogenic acid ameliorates endotoxin-induced liver injury by promoting mitochondrial oxidative phosphorylation. Biochem Biophys Res Commun 2016; 4: 1083–1089.
27. Wu D et al. Chlorogenic acid protects against cholestatic liver injury in rats. J Pharmacol Sci 2015; 3: 177–182.
28. Ding Y et al. Exploration of Emodin to treat alpha-naphthylisothiocyanateinduced cholestatic hepatitis via anti-inflammatory pathway. Eur J Pharmacol 2008; 1–3: 377–386.
29. Liu A et al. Saikosaponin d protects against acetaminophen-induced hepatotoxicity by inhibiting NF-kappaB and STAT3 signaling. Chem Biol Interactm 2014; 223C: 80–86.
30. Wang Y et al. Hepato-protective effect of resveratrol against acetaminopheninduced liver injury is associated with inhibition of CYP-mediated bioactivation and regulation of SIRT1-p53 signaling pathways. Toxicol Lett 2015; 2: 82–89.
31. Zhang J et al. Ginsenosides regulate PXR/NF-kappaB signaling and attenuate dextran sulfate sodium-induced colitis. Drug Metab Dispos 2015; 8: 1181–1189.
32. Xie W et al. Hepatoprotective effect of isoquercitrin against acetaminopheninduced liver injury. Life Sci 2016; 152: 180–189. [PubMed: 27049115]
33. Chen S et al. Plumbagin ameliorates CCl 4-induced hepatic fibrosis in rats via the epidermal growth factor receptor signaling pathway. Evid Based Complement Alternat Med 2015; 2015: 645727. [PubMed: 26550019]
34. Ohta Y et al. Melatonin attenuates disruption of serum cholesterol status in rats with a single alpha-naphthylisothiocyanate treatment. J Pineal Res 2007; 2: 159–165.
35. Cui YJ et al. Compensatory induction of liver efflux transporters in response to ANIT-induced liver injury is impaired in FXR-null mice. Toxicol Sci 2009; 1: 47–60.
36. Chawla A et al. “Don’t know much bile-ology”. Cell 2000; 1: 1–4.
37. Goodwin B et al. A regulatory cascade of the nuclear receptors FXR, SHP-1, and LRH-1 represses bile acid biosynthesis. Mol Cell 2000; 3: 517–526.
38. Zeng L et al. Simultaneous multicomponent quantitation of Chinese herbal injection Yin-zhi-huang in rat plasma by using a single-tube extraction procedure for mass spectrometry-based pharmacokinetic measurement. J Chromatogr B Analyt Technol Biomed Life Sci 2014; 967: 245–254.
39. Xu Y et al. Protective effects of chlorogenic acid on acute hepatotoxicity induced by lipopolysaccharide in mice. Inflamm Res 2010; 10: 871–877.
40. Shi H et al. Chlorogenic acid against carbon tetrachloride-induced liver fibrosis in rats. Eur J Pharmacol 2009; 1–3: 119–124.
41. Zhao Y et al. Paeoniflorin protectsagainst ANIT-induced cholestasis by ameliorating oxidative stress in rats. Food Chem Toxicol 2013; 58: 242–248. [PubMed: 23623840]
42. del Castillo-Olivares A, Gil G. Suppression of sterol 12alpha-hydroxylase transcription by the short heterodimer partner: insights into the repression mechanism. Nucleic Acids Res 2001; 19: 4035–4042.
43. Denson LA et al. The orphan nuclear receptor, shp, mediates bile acid-induced inhibition of the rat bile acid transporter, ntcp. Gastroenterology 2001; 1: 140–147.
44. Tanaka Y et al. ANIT-induced intrahepatic cholestasis alters hepatobiliary transporter expression via Nrf2- dependent and independent signaling. Toxicol Sci 2009; 2: 247–257.
45. Hishinuma I et al. Involvement of tumor necrosis factor-alpha in development of hepatic injury in galactosamine- sensitized mice. Hepatology 1990; 5: 1187–1191.
46. Scheiermann P et al. Application of interleukin-22 mediates protection in experimental acetaminophen-induced acute liver injury. Am J Pathol 2013; 4: 1107–1113.

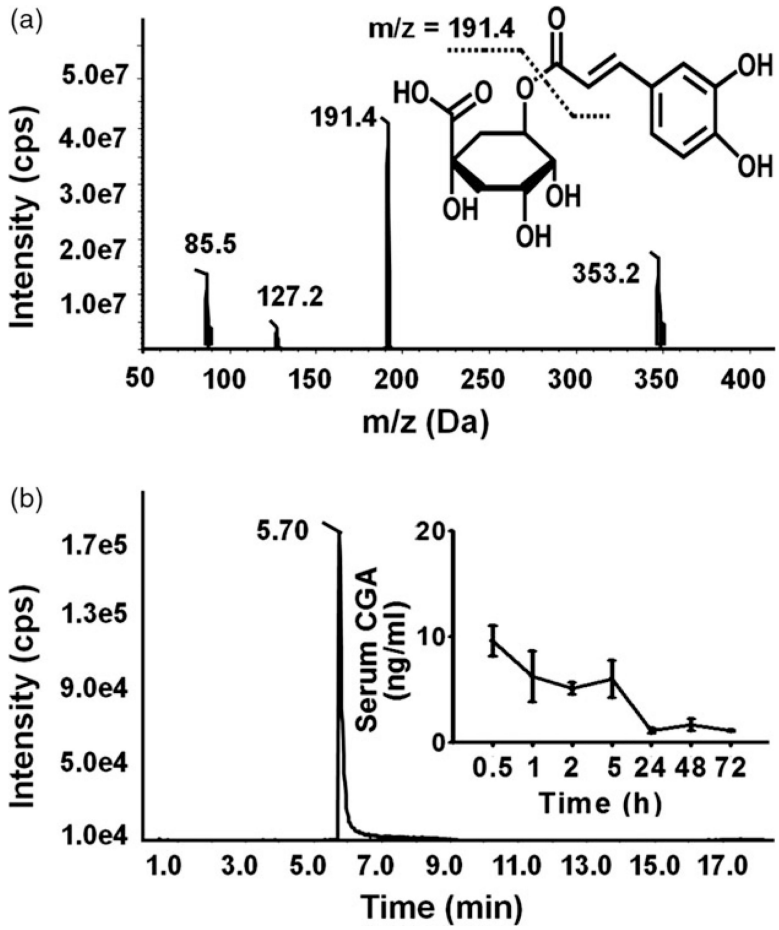


**Figure 1.**

Structure of CGA and its monitored systemic exposure level in the mice challenged with CGA 50 mg/kg for 5 days. (a) Fragmentation profile of CGA and Chemical structures of CGA. (b) The retention time and the serum concentrations of CGA after administration at 0.5, 1, 2, 5, 24 and 48 h.

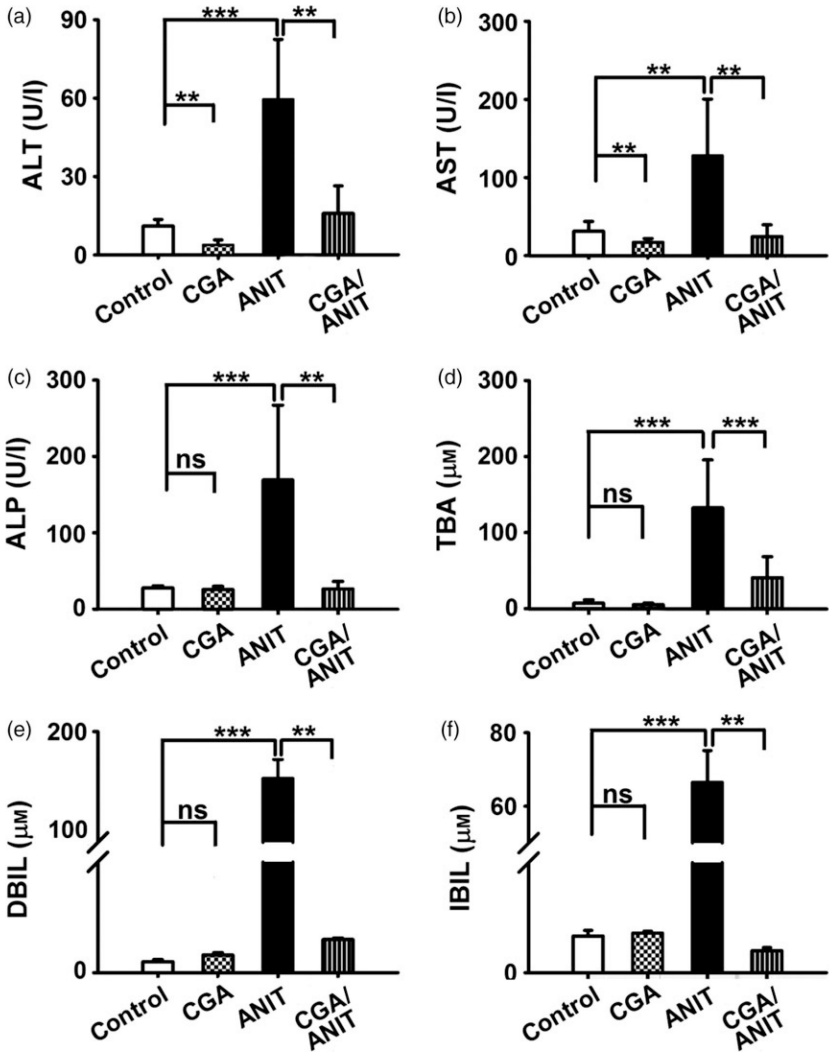


**Figue 2.**

Effects of CGA on the levels of serum ALT (a), AST (b), ALP (c), TBA (d), DBIL (e), IBIL (f) at 48 h after ANIT treatment in male mice. CGA was administered intragastrically once daily three 4 days prior to treatment with 75 mg/kg ANIT. Data are represented as means ± SD ($n = 5$; $^{**}P < 0.01$; $^{***}P < 0.001$; ns, not significant).

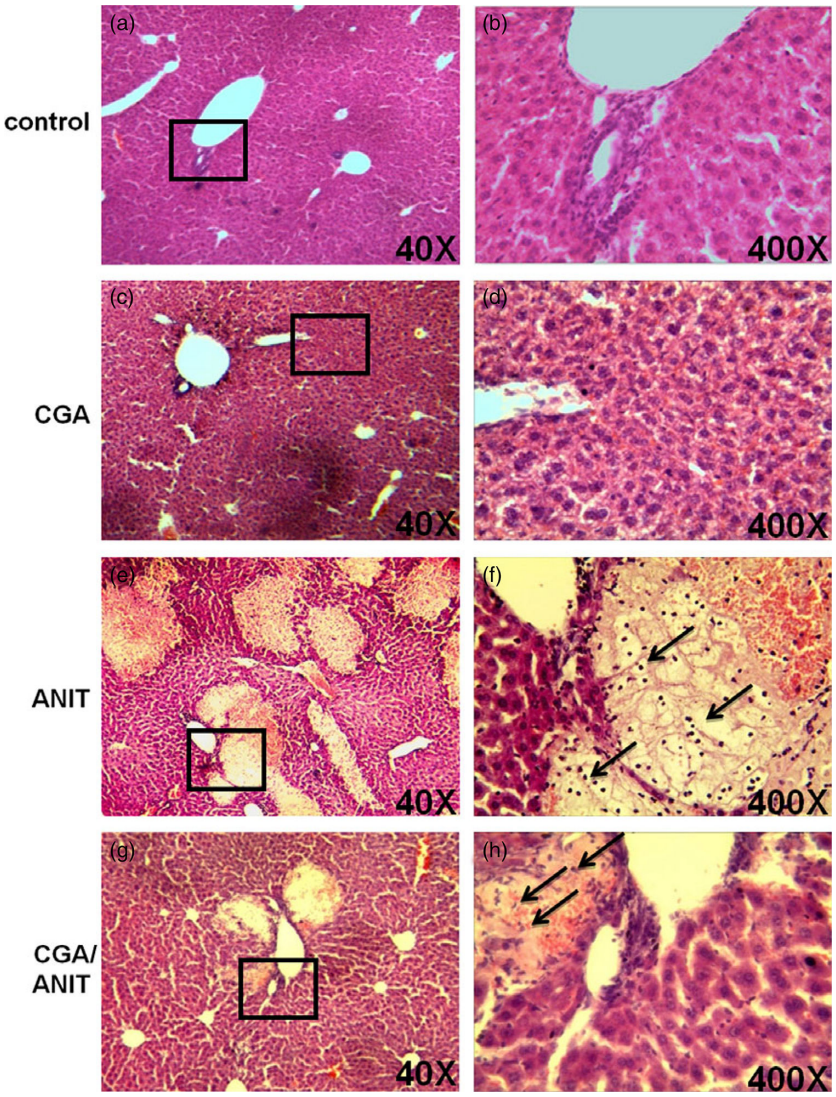


**Figure 3.**

Representative histological analysis of the livers in mice treated with ANIT and/or CGA. The patches framed in the pictures in the left column for each group were magnified pictures of the corresponding right column. CGA was administered to non-fasted mice by intragastrically once daily for 3 days prior to treatment with ANIT 75 mg/kg.

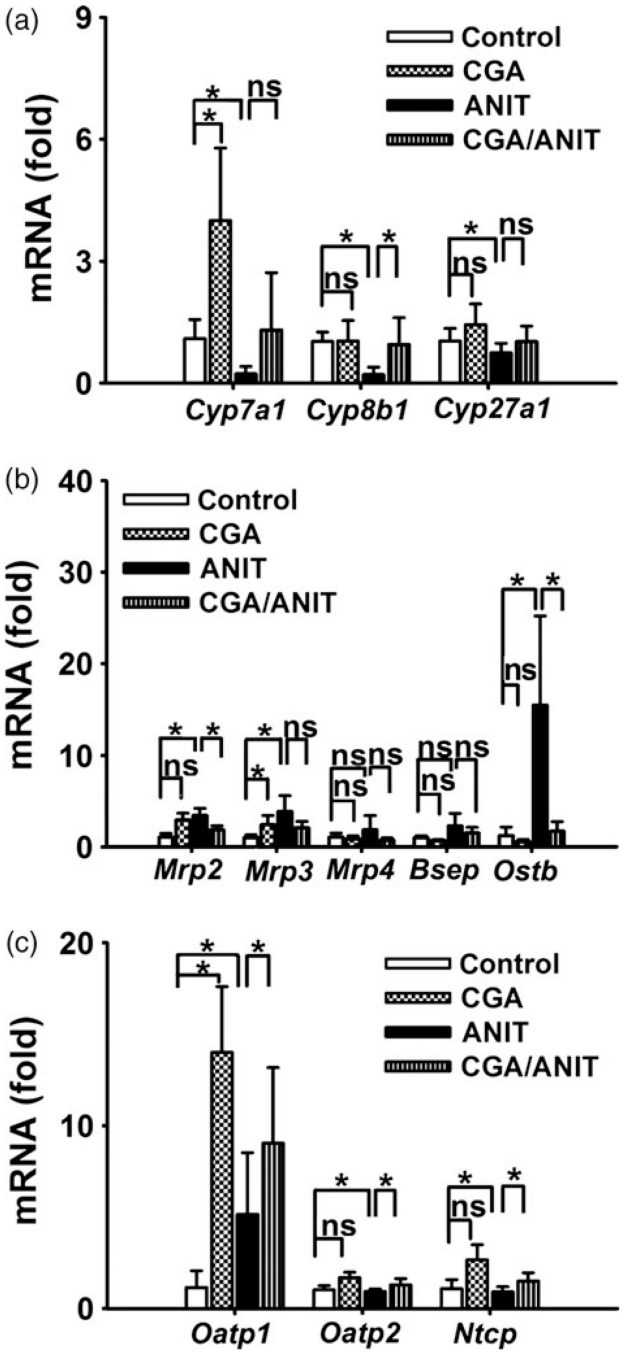


**Figure 4.**

Effects of CGA expression of mRNA from genes related to bile acid metabolism and transport in mouse liver. (a) Cyp7a1, Cyp8b1, Cyp27a1 mRNA. (b) The mRNA expressions of efflux and canalicular efflux transporters. (c) mRNA expressions of basolateral uptake transporters. Data are presented as mean ± SD. Asterisks indicate statistically significant differences between vehicle/control and CGA/control or vehicle/ANIT and CGA/ANIT treated male mice ($n = 5$; $*P < 0.05$; ns, not significant).

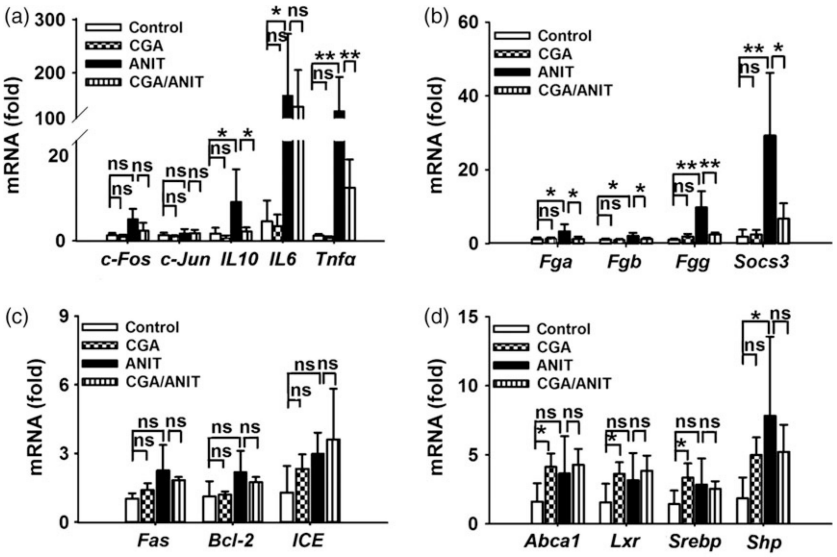


**Figure 5.**

Levels of mRNAs encoding by inflammation-related factors, apoptosis and necrosis-related factors, STAT3 target genes and LXR targrt genes. (a) c-Fos, c-Jun, Il-10, Il-6, Tnf-α. (b) Socs3, Fga, Fgb, Fgg. (c) Fas, Bcl-2, ICE. (d) Abca1, LXR, SREBP,SHP mRNAs. Data were from liver samples collected 48 h after ANIT treatment. The mRNA levels were measured by Q-PCR and normalized by 18S rRNA. Messenger RNA levels in vehicle-treated control mice were arbitrarily set as 1 and results were expressed as mean ± SD ($n = 5$; *$P < 0.05$; **$P < 0.01$; ns, not significant).

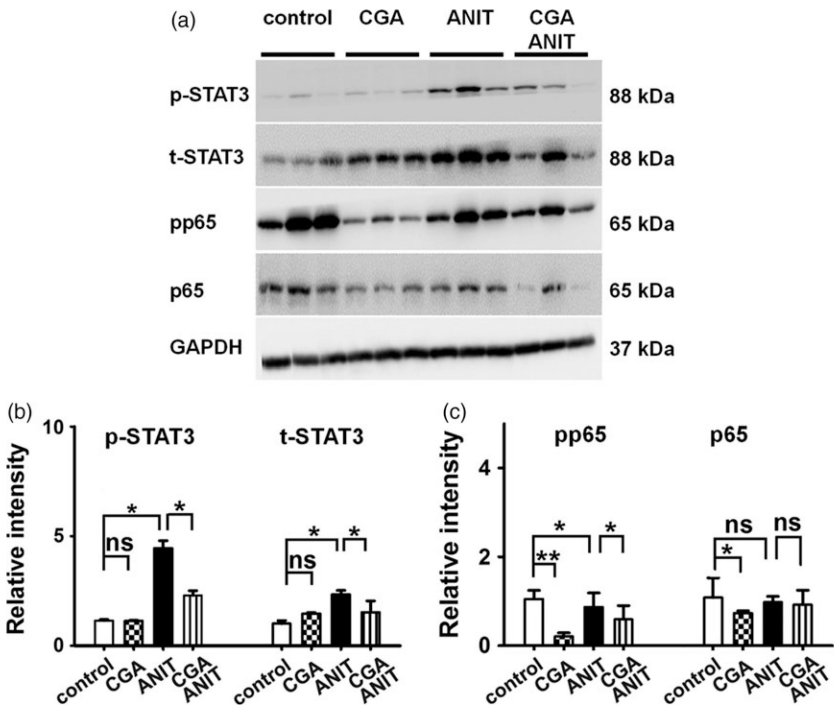


**Figure 6.**

Western blot and densitometry analysis of STAT3 and NFκB in liver extracts. Liver samples were collected 48 h after vehicle/ANIT treatment and three of them were randomly selected for protein analysis. GAPDH was used as a loading control. The molecular weight was indicated at the left side of the respective band. (a) Western blot of STAT3 and NFκB in liver extracts. (b) Densitometry analysis of STAT3 activation in liver extracts. (c) Densitometry analysis of NFκB activation in liver extracts. Results of control group were set as 1 and data were expressed as relative intensity of p-p65 and p-STAT3 vs p65 and STAT3 respectively ($n = 3$; $*P < 0.05$; $**P < 0.01$; ns, not significant).

**Table 1**

The sequences of the primers used in the Q-PCR in this study

| Genes | Forward primers | Reverse primers | Product (bp) |
|---|---|---|---|
| *Cyp7a1* | GTCCGGATATTCAAGGATGC | GGGAATGCCATTTACTTGGA | 107 |
| *Cyp8b1* | GATAGGGGAAGAGAGCCACC | TCCTCAGGGTGGTACAGGAG | 96 |
| *Cyp27a1* | GGGCACTAGCCAGATTCACA | CTATGTGCTGCACTTGCCC | 107 |
| *Mrp2* | TCTGTGAGTGCAAGAGACAGGT | TCCAGGACCAAGAGATTTGC | 107 |
| *Mrp3* | CTGCCGGCTAATTCAAATGT | TTGTGGAAGAATGTTGCCTC | 92 |
| *Mrp4* | TTAGATGGGCCTCTGGTTCT | GCCCACAATTCCAACCTTT | 102 |
| *Bsep* | AAGGACAGCCACACCAACTC | CCAGAACATGACAAACGGAA | 100 |
| *Ostb* | CCAGGACCAGGATGGAATAA | AGAGAAAGCTGCAGCCAATG | 110 |
| *Oatp1* | TAATCGGGCCAACAATCTTC | ACTCCCATAATGCCCTTGG | 109 |
| *Oatp2* | TAGCTGAATGAGAGGGCTGC | ACCAAACTCAGCATCCAAGC | 103 |
| *Ntcp* | TCCGTCGTAGATTCCTTTGC | AGGGGGACATGAACCTCAG | 96 |
| *c-Fos* | TGGCACTAGAGACGGACAGA | TCCTACTACCATTCCCCAGC | 94 |
| *c-Jun* | GGGACACAGCTTTCACCCTA | GAAAAGTAGCCCCCAACCTC | 104 |
| *IL10* | TGTCAAATTCATTCATGGCCT | ATCGATTTCTCCCCTGTGAA | 108 |
| *IL6* | ACCAGAGGAAATTTTCAATAGC | TGATGCACTTGCAGAAAACA | 109 |
| *Tnfα* | AGGGTCTGGGCCATAGAACT | CCACCACGCTCTTCTGTCTAC | 103 |
| *Fas* | CCTCAGCTTTAAACTCTCGGA | CAGACATGCTGTGGATCTGG | 107 |
| *Bcl-2* | GGTCTTCAGAGACAGCCAGG | GATCCAGGATAACGGAGGCT | 94 |
| *ICE* | TGGAAATGTGCCATCTTCTTT | TCAGCTCCATCAGCTGAAAC | 108 |
| *Fga* | CAACTCTTGGGCCACGTACT | GGGTCACCTGCCTCATCTT | 108 |
| *Fgb* | AGGAGGCTCTTCCTTTCTCC | CAAGCTGCCGATGATGACTA | 90 |
| *Fgg* | TCAAGCTGGGCTACCTTCTG | AACCCACGAGACAAGCATTC | 93 |
| *Socs3* | AACTTGCTGTGGGTGACCAT | AAGGCCGGAGATTTCGCT | 136 |
| *Abca1* | GCTGCAGGAATCCAGAGAAT | CATGCACAAGGTCCTGAGAA | 107 |
| *Srebp* | TGGTTGTTGATGAGCTGGAG | GGCTCTGGAACAGACACTGG | 96 |
| *Lxr* | TGGAGAACTCAAAGATGGGG | TGAGAGCATCACCTTCCTCA | 106 |
| *Shp* | AAGACTTCACACAGTGCCCA | CACGATCCTCTTCAACCCAG | 107 |

*J Pharm Pharmacol*. Author manuscript; available in PMC 2018 December 20.